



Trans. Nonferrous Met. Soc. China 33(2023) 576-583

Transactions of Nonferrous Metals Society of China

www.tnmsc.cn



# Improvement of utilization efficiency of magnesite by (NH<sub>4</sub>)<sub>2</sub>SO<sub>4</sub> roasting—water leaching process

Xiao-yi SHEN<sup>1,2</sup>, Yan-xiang HUANG<sup>1</sup>, Hong-mei SHAO<sup>3</sup>, Yan LIU<sup>1</sup>, Hui-min GU<sup>1,2</sup>, Yu-chun ZHAI<sup>1</sup>

- 1. Key Laboratory for Ecological Metallurgy of Multimetallic Mineral (Ministry of Education), School of Metallurgy, Northeastern University, Shenyang 110819, China;
  - 2. Liaoning Key Laboratory for Metallurgical Sensor and Technology, Northeastern University, Shenyang 110819, China;
- 3. School of Environmental and Chemical Engineering, Shenyang Ligong University, Shenyang 110159, China

Received 5 October 2021; accepted 6 March 2022

**Abstract:**  $(NH_4)_2SO_4$  roasting—water leaching process was studied as a method for improving the utilization efficiency of magnesite. Transformation of the mineral phases during roasting was evaluated by X-ray diffraction (XRD) analysis, combined with thermogravimetry—differential thermal analysis (TG-DTA). The data were compared with the phase transformation of MgO during roasting using  $(NH_4)_2SO_4$ . The experimental results demonstrated that at a  $(NH_4)_2SO_4$ / magnesite (MgO in ore) molar ratio of 1.6:1, roasting temperature of 475 °C, and roasting time of 2 h using a particle size of ~74 µm, the magnesium extraction rate reached a maximum of 98.7%. The phase transformation during roasting could be summarized as follows: MgCO<sub>3</sub> was transformed into  $(NH_4)_2Mg_2(SO_4)_3$ , and then decomposed into MgSO<sub>4</sub>. The reaction followed the mixed control mechanism involving chemical reaction control and diffusion control, with an apparent activation energy of 33.02 kJ/mol.

Key words: magnesite; (NH<sub>4</sub>)<sub>2</sub>SO<sub>4</sub> roasting-water leaching method; reaction process; phase transformation

# 1 Introduction

Magnesite is considered to be one of the most suitable mineral resources for producing various magnesium compounds and metal magnesium [1]. China is particularly rich in magnesite deposits, especially in Liaoning Province. For a long time, high-grade magnesite has mainly been used to produce caustic calcined magnesia, dead burned magnesia, and fused magnesia, which are used primarily as refractory materials [2]. Caustic calcined magnesia can be used to produce various chemical products, such as Mg(OH)<sub>2</sub>, an important fine chemical that is widely applied as a neutralizer for acids and flue gases, as a flame retardant, as a sorbent for heavy metal ions in wastewater, and as a

precursor of MgO [1,3]. Mg(OH)<sub>2</sub> can be prepared from caustic calcined magnesia by the direct hydration method, but the impurities cannot be removed, resulting in a low-value Mg(OH)<sub>2</sub> product [4,5]. Another viable method for producing Mg(OH)<sub>2</sub> is acid leaching followed by purification and precipitation using an alkali, such as NaOH, Ca(OH)<sub>2</sub>, or ammonia. The inorganic acid used in the process, such as H<sub>2</sub>SO<sub>4</sub>, HNO<sub>3</sub>, or HCl, has a strong corrosive effect on the equipment [5,6].

Long-term disorderly utilization of ores has led to a decrease in the grade of magnesite and a large amount of waste low-grade magnesite [7–9]. Besides the waste of resources, the dumped waste magnesite poses a serious threat to the environment [8]. Thus, developing an efficient and feasible technique for dealing with magnesite at

varying concentrations is a pressing task for enhancing the efficiency of resource utilization and environmental sustainability. The (NH<sub>4</sub>)<sub>2</sub>SO<sub>4</sub> roasting-water leaching process is an efficient route for extracting valuable metals and can be carried out at low temperature [10]. This method has been used to process coal fly ash [11], zinc oxide ore and zinc leaching residue [12], Ti-bearing blast furnace slag [13], spent lithium nickel cobalt manganese oxides [14], nickel oxide ore [15], mixed oxidesulfide nickel ore [16], nickel-chromium mixed oxidized ore [10], and so on. Although the (NH<sub>4</sub>)<sub>2</sub>SO<sub>4</sub> roasting-water leaching process has been used to treat caustic calcined magnesia [17], the two heating processes are energy intensive. Therefore, the (NH<sub>4</sub>)<sub>2</sub>SO<sub>4</sub> roasting-water leaching process was adopted to treat magnesite to realize the efficient utilization of magnesite. Firstly, the fine magnesite was mixed uniformly with (NH<sub>4</sub>)<sub>2</sub>SO<sub>4</sub>, followed by roasting. After water leaching and filtration, magnesium entered the filtrate and was separated from quartz. The roasting gas was used to recovery (NH<sub>4</sub>)<sub>2</sub>SO<sub>4</sub> and ammonia. Subsequently, the purified filtrate was used to prepare Mg(OH)<sub>2</sub> by employing recycled ammonia. The resulting NH<sub>3</sub> and CO<sub>2</sub> can also be used to produce urea and ammonium bicarbonate, which are two fertilizers used in large quantities. In this case, a certain amount of ammonia is needed to later precipitate Mg(OH)<sub>2</sub>.

In this investigation, a typical magnesite from Dashiqiao located in northeast China was roasted with industrial (NH<sub>4</sub>)<sub>2</sub>SO<sub>4</sub> and then leached with water. This study provides a better understanding of the key parameters for optimizing magnesite roasting. The influences of variables, such as the particle size, (NH<sub>4</sub>)<sub>2</sub>SO<sub>4</sub>/magnesite (MgO in ore) molar ratio, roasting temperature, and time on magnesium extraction, were studied. The phase transformation and reactivity of magnesium compounds during roasting were identified by X-ray diffraction (XRD) analysis, combined with thermogravimetry-differential thermal (TG-DTA). Finally, a reaction mechanism was proposed.

# 2 Experimental

# 2.1 Materials

Magnesite from Dashiqiao, Liaoning Province, China, was ground to a particle size of 74–250 µm

and used as the raw material. Industrial grade (NH<sub>4</sub>)<sub>2</sub>SO<sub>4</sub> was served as the reactant and used asreceived.

#### 2.2 Procedure

A vertical resistance furnace (temperature accuracy of ±1 °C) was employed in experiments. Fine magnesite (50 g) and a specific amount of (NH<sub>4</sub>)<sub>2</sub>SO<sub>4</sub> to provide a molar ratio from 1.1:1 to 1.7:1 were uniformly mixed, placed into a corundum crucible, and roasted in a furnace for a period of time within 2.5 h at preset temperatures ranging from 400 to 525 °C. The specimens were then taken out and leached with water at 80 °C for 1 h at a liquid/solid ratio of 4:1. Leaching residue with a mass from 1.78 to 13.56 g was obtained after filtration, washing, and drying. For the kinetics investigation, once the temperature reached the required value of 425-475 °C, the specimens were collected at a preset time interval of 10 min, cooled rapidly, and water leached at 80 °C for 1 h before analysis.

The concentration of Mg was determined by titration with ethylenediamine tetraacetic acid (EDTA). The extraction rate of magnesium was determined using Eq. (1):

$$\eta = \frac{Vc}{mw} \times 100\% \tag{1}$$

where  $\eta$  is the extraction rate of magnesium, %; V is the volume of the leaching solution, L; c is the magnesium concentration, g/L; m is the mass of magnesite, g; and w is the mass fraction of magnesium in the magnesite, %.

#### 3 Results and discussion

#### 3.1 Magnesite characterization

The main components in magnesite are listed in Table 1 based on the analysis by the chemical method. Figure 1 shows the XRD pattern and scanning electron microscopy (SEM) image of the fine magnesite. As the main component, the content of MgO was 45.58 wt.%, which was mainly in the form of MgCO<sub>3</sub>. Fe<sub>2</sub>O<sub>3</sub>, SiO<sub>2</sub>, and CaO were present in low grades of 0.32, 1.96, and 0.46 wt.%, respectively. The other 51.68 wt.% of the ore mainly comprised CO<sub>2</sub> from MgCO<sub>3</sub>. The XRD study indicated that magnesite was the major mineral phase and quartz was the minor phase. The magnesite particles were uneven and irregular.

**Table 1** Main chemical components of magnesite (wt.%)

MgO	$Fe_2O_3$	$SiO_2$	CaO
45.58	0.32	1.96	0.46

# 3.2 Influence of roasting parameters

# 3.2.1 Particle size

To ascertain the influence of the particle size on the magnesium extraction, experiments were performed using a (NH<sub>4</sub>)<sub>2</sub>SO<sub>4</sub>/magnesite molar ratio of 1.5:1, where the sample was roasted at 450 °C for 2 h. The data in Fig. 2(a) show that the amount

of magnesium extracted decreased as the magnesite particle size increased. The magnesium extraction rate was 94.1% at a particle size of ~74  $\mu$ m. Smaller particles improved the probability for contact of the reactants in the gas–liquid–solid reactions [10]. However, an overly small particle size significantly increased the energy consumption. A particle size of ~74  $\mu$ m was selected and used in the subsequent experiments.

# 3.2.2 Molar ratio of (NH<sub>4</sub>)<sub>2</sub>SO<sub>4</sub>/magnesite

To determine the influence of the (NH<sub>4</sub>)<sub>2</sub>SO<sub>4</sub>/ magnesite molar ratio on magnesium extraction, the

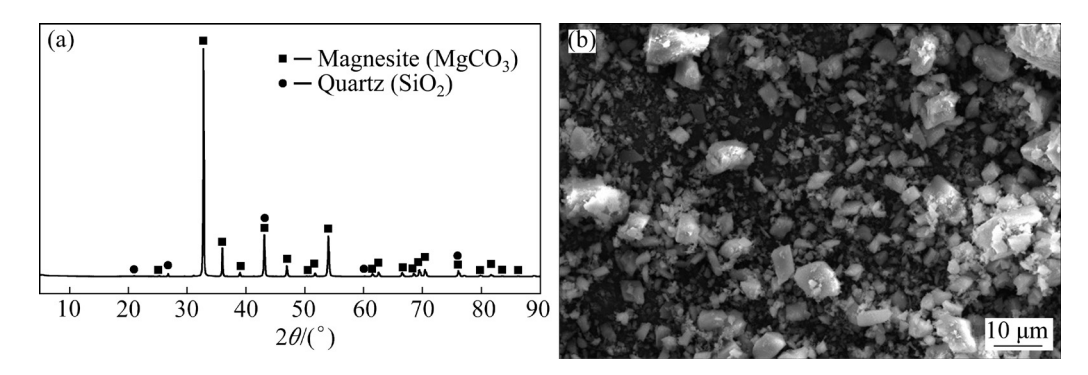


Fig. 1 XRD pattern (a) and SEM image (b) of magnesite

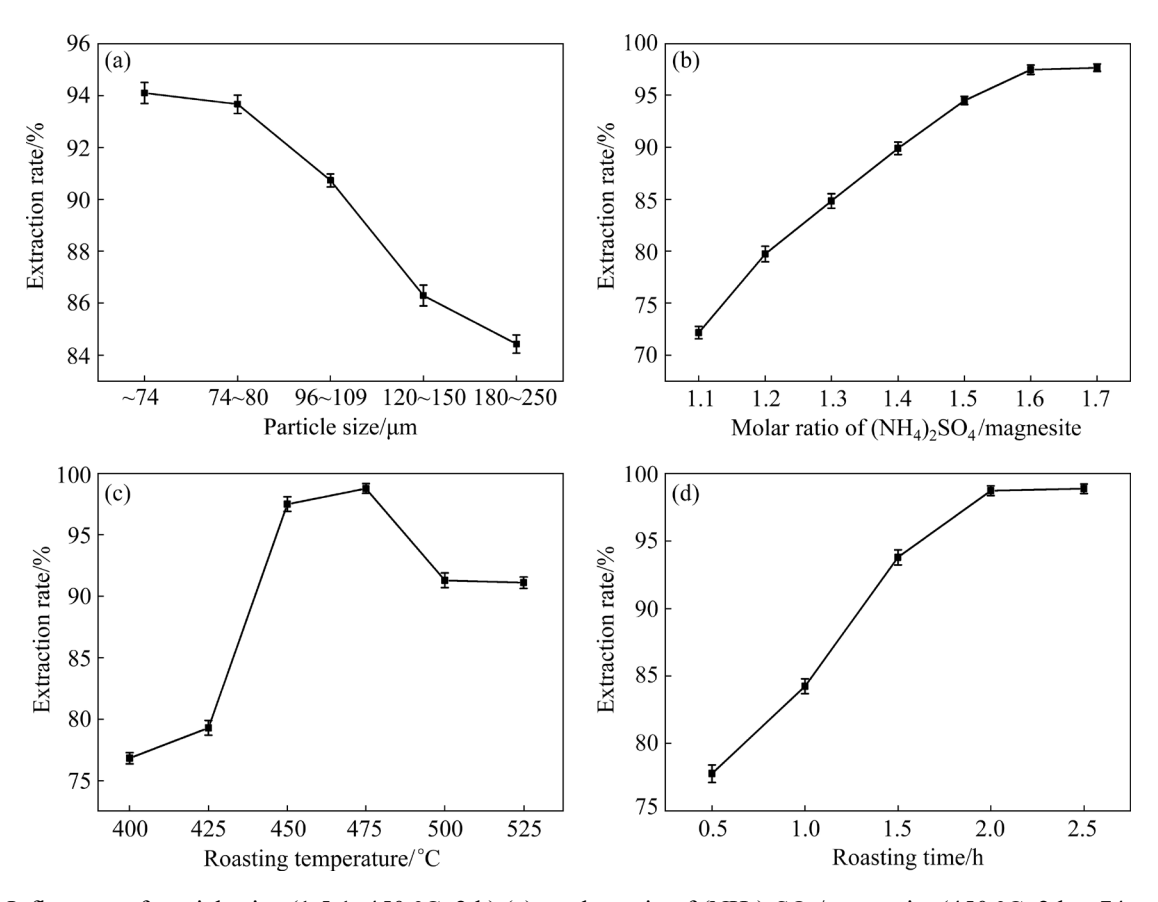


Fig. 2 Influences of particle size (1.5:1, 450 °C, 2 h) (a), molar ratio of (NH<sub>4</sub>)<sub>2</sub>SO<sub>4</sub>/magnesite (450 °C, 2 h,  $\sim$ 74 µm) (b), roasting temperature (1.6:1, 2 h,  $\sim$ 74 µm) (c), and roasting time (475 °C, 1.6:1,  $\sim$ 74 µm) (d) on Mg extraction rate

ore sample with a particle size of  $\sim$ 74 µm was roasted at 450 °C for 2 h. Increasing the molar ratio had an appreciable impact on the magnesium extraction (Fig. 2(b)). The magnesium extraction rate increased from 72.1% at a molar ratio of 1.1:1 to 97.5% at a molar ratio of 1.6:1. Thereafter, the magnesium extraction rate showed no obvious increase. Sufficient (NH<sub>4</sub>)<sub>2</sub>SO<sub>4</sub> is necessary to achieve high magnesium extraction rate (NH<sub>4</sub>)<sub>2</sub>SO<sub>4</sub> improves the interaction between the reactants, thereby expanding the contact area as the dosage of (NH<sub>4</sub>)<sub>2</sub>SO<sub>4</sub> increases. However, excessive (NH<sub>4</sub>)<sub>2</sub>SO<sub>4</sub> can not only lead to the excessive consumption of auxiliary materials, but also increase the energy consumption. The molar ratio of 1.6:1 was chosen in subsequent experiments.

#### 3.2.3 Roasting temperature

The influence of the roasting temperature on magnesium extraction was studied by varying the roasting temperature in the range of 400-525 °C; the sample was roasted for 2 h at a molar ratio of 1.6:1 using an ore particle size of  $\sim$ 74 µm. The roasting temperature exerted a significant effect on magnesium extraction (Fig. 2(c)). The magnesium extraction rate increased from 76.8% at 400 °C to 98.7% at 475 °C. Thereafter, a sharp decrease in the magnesium extraction rate was observed. This result suggests that a temperature of 475 °C is advisable for magnesium extraction. Increasing temperature facilitates the roasting reaction, but an excessively high temperature has a negative effect on magnesium extraction. This result is explained as follows: (NH<sub>4</sub>)<sub>2</sub>SO<sub>4</sub> is decomposed during roasting and is even decomposed into N<sub>2</sub>, SO<sub>2</sub>, H<sub>2</sub>O, and NH<sub>3</sub> at high temperatures [18,19]. Thus, the complete decomposition of (NH<sub>4</sub>)<sub>2</sub>SO<sub>4</sub> can presumably reduce the effective dosage of the reaction medium.

# 3.2.4 Roasting time

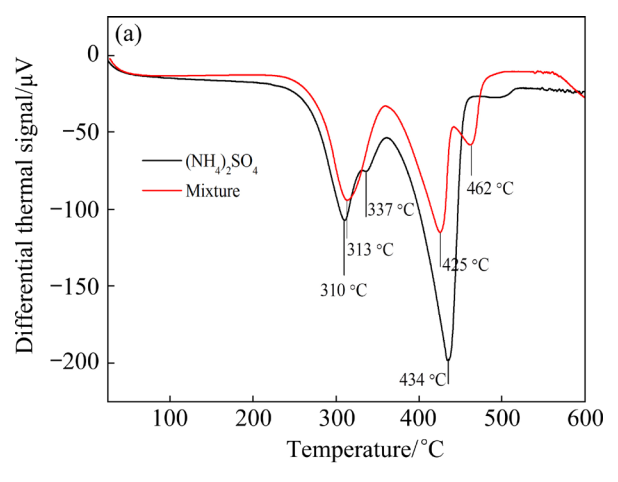
The influence of the roasting time on magnesium extraction was investigated at 475 °C, using a molar ratio of 1.6:1 and ore particle size of ~74 μm. The magnesium extraction rate increased obviously within 2 h; thereafter, a plateau was observed at extended time (Fig. 2(d)). A maximum magnesium extraction rate of 98.7% was obtained after roasting for 2 h. The roasting time was less than that used in roasting caustic calcined magnesia using (NH<sub>4</sub>)<sub>2</sub>SO<sub>4</sub> [17]. Prolonging the roasting time led to decreased efficiency and increased energy

consumption. A roasting time of 2 h was considered suitable

It could be concluded that the appropriate roasting parameters were as follows:  $(NH_4)_2SO_4/$  magnesite molar ratio of 1.6:1, roasting temperature of 475 °C, roasting time of 2 h, and particle size of  $\sim$ 74  $\mu$ m.

#### 3.3 Roasting process

To confirm the success of the roasting process, TG–DTA technique was used to monitor the decomposition of (NH<sub>4</sub>)<sub>2</sub>SO<sub>4</sub> and the mixture of magnesite and (NH<sub>4</sub>)<sub>2</sub>SO<sub>4</sub>. Figure 3 shows the representative TG–DTA curves in the temperature range of 25–600 °C, obtained at a heating rate of 10 K/min under air flow at a rate of 100 mL/min. In the DTA curve of (NH<sub>4</sub>)<sub>2</sub>SO<sub>4</sub> (Fig. 3(a)), three distinct endothermic peaks were observed at 310, 337, and 434 °C, corresponding to the three distinct mass losses of 12.81%, 6.12%, and 80.56% in the TG curve in the temperature ranges of 250–325, 325–350, and 350–460 °C, respectively. The three



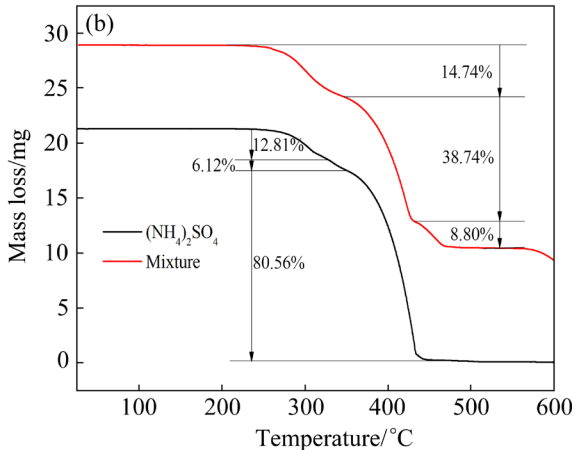


Fig. 3 DTA (a) and TG (b) curves of  $(NH_4)_2SO_4$  and mixture of magnesite and  $(NH_4)_2SO_4$ 

distinct mass losses were extremely close to the stoichiometric loss of NH<sub>3</sub> from (NH<sub>4</sub>)<sub>2</sub>SO<sub>4</sub> (12.88%), loss of H<sub>2</sub>O via (NH<sub>4</sub>)<sub>2</sub>S<sub>2</sub>O<sub>7</sub> formation (7.82%), and total decomposition of (NH<sub>4</sub>)<sub>2</sub>SO<sub>4</sub> (79.29%). Thus, the three distinct mass losses were respectively assigned to the decomposition of (NH<sub>4</sub>)<sub>2</sub>SO<sub>4</sub>, NH<sub>4</sub>HSO<sub>4</sub>, and (NH<sub>4</sub>)<sub>2</sub>S<sub>2</sub>O<sub>7</sub>, which are summarized as Reactions (2)-(4), respectively [18,19]. LI et al [18] and ZHANG et al [19] studied the decomposition of (NH<sub>4</sub>)<sub>2</sub>SO<sub>4</sub> in detail. LI et al [18] reported that a large amount of NH3 was released at 384 °C and a large amount of SO<sub>2</sub> and H<sub>2</sub>O were emitted at 520 °C. YIN et al [20] reported that the most significant mass loss was in the temperature range of 450-520 °C due to the total decomposition of  $(NH_4)_2SO_4$ .

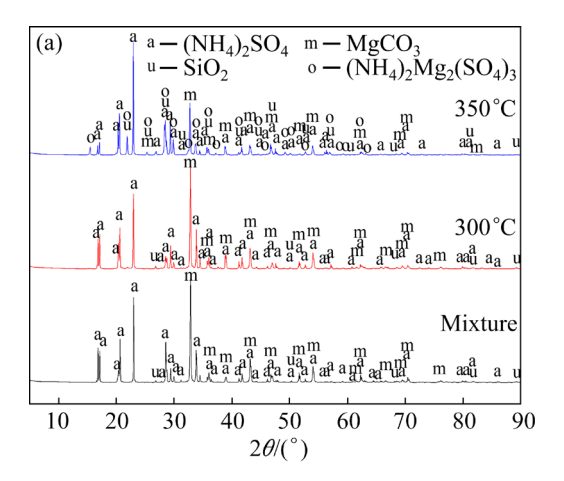
$$(NH4)2SO4 \rightarrow NH3 \uparrow +NH4HSO4$$
 (2)

$$2NH_4HSO_4 \rightarrow (NH_4)_2S_2O_7 + H_2O \tag{3}$$

$$3(NH_4)_2S_2O_7 \rightarrow 2NH_3 \uparrow +2N_2 \uparrow +9H_2O+6SO_2$$
 (4)

Three obvious endothermic peaks appeared at approximately 313, 425, and 462 °C in the DTA curve of the mixture, accompanied by three prominent mass losses in the TG curve of 14.74%, 38.74%, and 8.80% in the temperature ranges of 250–350, 350–430, and 430–485 °C, respectively. The first mass loss is ascribed mainly to (NH<sub>4</sub>)<sub>2</sub>SO<sub>4</sub> decomposition, but the second and the third mass losses were complex, involving the synthesis and deamination of metal ammonium sulfates [10]. The peak at 336 °C disappeared because of rapid reaction between NH<sub>4</sub>HSO<sub>4</sub> and MgCO<sub>3</sub> [20].

further clearly identify the phase transformation during roasting, XRD analysis was also employed to identify the phase structures of the specimens roasted at different temperatures, as shown in Fig. 4. There was little difference between the diffraction peaks of the specimens obtained at 300 °C and the initial mixture, indicating that the reaction did not progress substantially. Due to the strong diffraction peaks of MgCO<sub>3</sub> and (NH<sub>4</sub>)<sub>2</sub>SO<sub>4</sub>, the diffraction peaks of quartz were not apparent. The dominant diffraction peaks in the profile of the specimen roasted at 350 °C corresponded to MgCO<sub>3</sub>, (NH<sub>4</sub>)<sub>2</sub>SO<sub>4</sub>, and (NH<sub>4</sub>)<sub>2</sub>Mg<sub>2</sub>(SO<sub>4</sub>)<sub>3</sub>. Thus, (NH<sub>4</sub>)<sub>2</sub>Mg<sub>2</sub>(SO<sub>4</sub>)<sub>3</sub> was synthesized, whereas the diffraction peaks of (NH<sub>4</sub>)<sub>2</sub>SO<sub>4</sub> and MgCO<sub>3</sub> became weaker. The main phases in the specimen roasted at 400 °C were (NH<sub>4</sub>)<sub>2</sub>Mg<sub>2</sub>(SO<sub>4</sub>)<sub>3</sub> and (NH<sub>4</sub>)<sub>2</sub>SO<sub>4</sub>. The diffraction peaks of MgCO<sub>3</sub> almost disappeared. The main phases in the specimen obtained at 450 °C were consistent with those in the specimen obtained at 400 °C. The main phases in the specimen roasted at 500 °C were (NH<sub>4</sub>)<sub>2</sub>Mg<sub>2</sub>(SO<sub>4</sub>)<sub>3</sub> and MgSO<sub>4</sub>, indicating that (NH<sub>4</sub>)<sub>2</sub>Mg<sub>2</sub>(SO<sub>4</sub>)<sub>3</sub> began to decompose into MgSO<sub>4</sub> below 500 °C. The diffraction peaks of NH<sub>4</sub>HSO<sub>4</sub> were indistinct during roasting due to the rapid reaction rate [20].



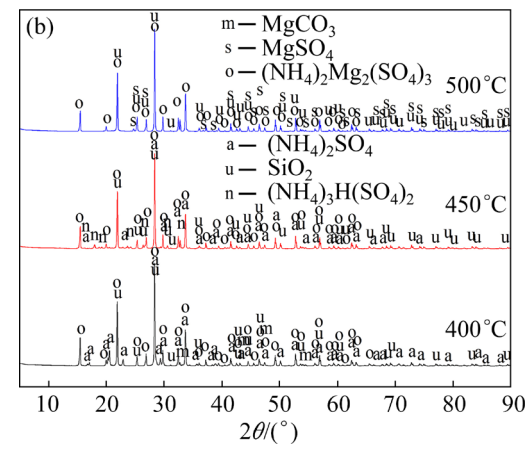


Fig. 4 XRD patterns of mixtures roasted at different temperatures

In order to further distinctly confirm the transformation of the magnesium compounds, a mixture of MgO and (NH<sub>4</sub>)<sub>2</sub>SO<sub>4</sub> was roasted at temperatures ranging from 250 to 550 °C and the phase structures of MgO and the roasted specimens were identified, as shown in Fig. 5. (NH<sub>4</sub>)<sub>2</sub>Mg<sub>2</sub>(SO<sub>4</sub>)<sub>3</sub> synthesis began below 300 °C and became extensive in the range of 400–500 °C. Further, (NH<sub>4</sub>)<sub>2</sub>Mg<sub>2</sub>(SO<sub>4</sub>)<sub>3</sub> began to transform into MgSO<sub>4</sub> below 500 °C; the process was completed below 550 °C. Thus, the second endothermic peak at 425 °C is mostly attributed to the extensive synthesis of (NH<sub>4</sub>)<sub>2</sub>Mg<sub>2</sub>(SO<sub>4</sub>)<sub>3</sub> and decomposition

of NH<sub>4</sub>HSO<sub>4</sub>. The peak at 462 °C is assigned to the formation of MgSO<sub>4</sub>.

#### 3.4 Mechanism

The magnesium extraction rate was plotted against the roasting time at different temperatures, as shown in Fig. 6(a). Increasing the roasting temperature and time gradually improved the magnesium extraction rate. As described by Eqs. (2)–(4), the decomposition of (NH<sub>4</sub>)<sub>2</sub>SO<sub>4</sub> progressed gradually to completion, whereas the reaction between NH<sub>4</sub>HSO<sub>4</sub> and the magnesium compound was quick [20]. During roasting in the temperature range of 425-475 °C, the roasted magnesite particles were composed of three parts from the external to the internal: the product layer where the completely formed product (metal ammonium sulfate) is deposited, the reaction layer where NH<sub>4</sub>HSO<sub>4</sub> reacts with magnesite, and the unreacted magnesite core. Thus, the steps governing the reaction between magnesite and decomposed NH<sub>4</sub>HSO<sub>4</sub> may include the diffusion of NH<sub>4</sub>HSO<sub>4</sub> through the solid product layer into the unreacted magnesite surface to form the reaction layer, the chemical reaction of magnesite with NH<sub>4</sub>HSO<sub>4</sub> in the reaction layer, and the diffusion of the reaction product. The reaction occurring during roasting is the typical gas–liquid–solid reaction. Thus, to evaluate the kinetic mechanism of this transformation, the constant conversion method, as described by Eq. (5), should be adopted rather than the shrinking unreacted core model [10,20].

$$\ln t^{-1} = \ln A - E_{\alpha}/(RT) \tag{5}$$

where t is the reaction time, min; A is the frequency factor, min<sup>-1</sup>;  $E_a$  is the apparent activation energy, kJ/mol; R is the molar gas constant, 8314 J/(mol·K); T is the thermodynamic temperature, K.

The plots of  $\ln t^{-1}$  versus 1/T in the temperature range from 698 to 748 K are presented in Fig. 6(b). From the slopes of the fitted lines, the value of the apparent activation energy was 33.02 kJ/mol, indicating a mixed control mechanism involving chemical reaction control and diffusion control.

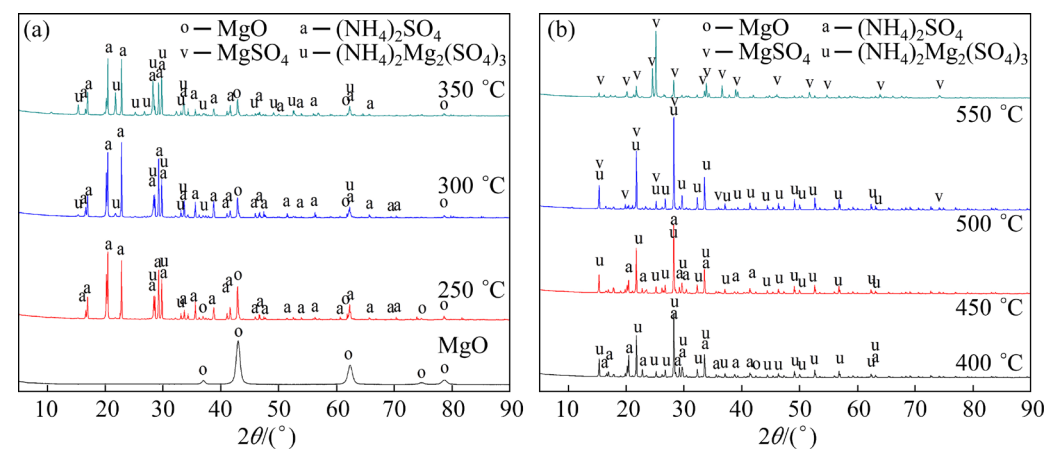


Fig. 5 XRD patterns of MgO and roasted specimens by (NH<sub>4</sub>)<sub>2</sub>SO<sub>4</sub> at different temperatures

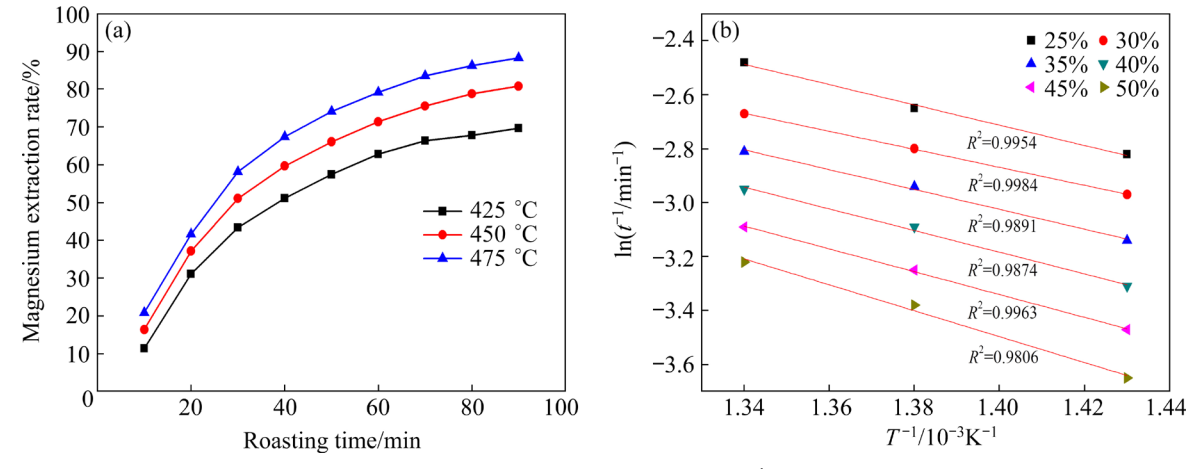


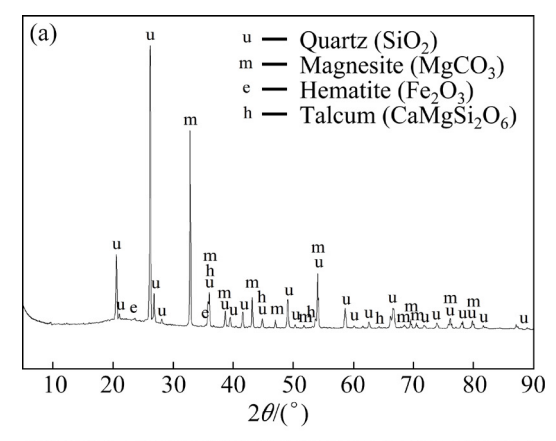
Fig. 6 Magnesium extraction rate versus roasting time (a) and plots of  $\ln t^{-1}$  versus 1/T (b) at different temperatures

#### 3.5 Characterization of leaching residue

The main components of the leaching residue obtained by applying the above appropriate roasting parameters were determined by the chemical method and are listed in Table 2. The contents of MgO, Fe<sub>2</sub>O<sub>3</sub>, SiO<sub>2</sub>, and CaO were 15.61, 4.21, 54.97, and 6.38 wt.%, respectively. The XRD pattern and SEM image presented in Fig. 7 indicated that the main phases in the residue were quartz and magnesite; hematite and talcum were more difficult to identify. The residue particles were irregular with a rough surface.

**Table 2** Main chemical components of leaching residue (wt.%)

MgO	$Fe_2O_3$	$SiO_2$	CaO
15.61	4.21	54.97	6.38



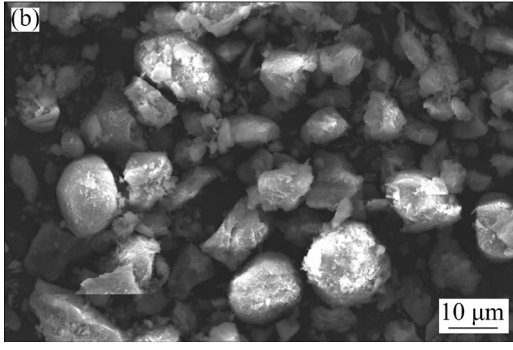


Fig. 7 XRD pattern (a) and SEM image (b) of leaching residue

# 4 Conclusions

(1) The  $(NH_4)_2SO_4$  roasting—water leaching process is efficient for treating magnesite. At a  $(NH_4)_2SO_4$ /magnesite molar ratio of 1.6:1, roasting temperature of 475 °C, roasting time of 2 h, and particle size of ~74 µm, the magnesium extraction

rate reached a maximum of 98.7%.

- (2) Kinetic study demonstrates that the roasting process conforms to the mixed control mechanism involving chemical reaction control and diffusion control, where the apparent activation energy is 33.02 kJ/mol.
- (3) Water and (NH<sub>4</sub>)<sub>2</sub>SO<sub>4</sub> can be cyclically utilized in the whole process. This process is a potential alternative method for processing magnesite.

# Acknowledgments

The authors appreciate financial supports from the National Natural Science Foundation of China (Nos. 51774070, 52004165), and the Science and Technology Project of Yunnan Province, China (No. 202101AS070029).

#### References

- RAZA N, ZAFAR Z I, NAJAM U H, KUMAR R V. Leaching of natural magnesite ore in succinic acid solutions
  International Journal of Mineral Processing, 2015, 139: 25-30.
- [2] LI Jin-hua, ZHANG Yun, SHAO Shuai, ZHANG Shu-shen, MA Shu-ming. Application of cleaner production in a Chinese magnesia refractory material plant [J]. Journal of Cleaner Production, 2016, 113: 1015–1023.
- [3] SHAO Hong-mei, CUI Yong, ZHANG Wei, XU Wen-di, LI Xue-tian, SHAO Zhong-cai. Preparation of flower-like Mg(OH)<sub>2</sub> from nickel laterite and its adsorption ability for Cu<sup>2+</sup> and Ni<sup>2+</sup> [J]. The Chinese Journal of Nonferrous Metals, 2021, 31(9): 2561–2572. (in Chinese)
- [4] GUO Hong-fan, XIE Jia-yang, HU Han, LI Xue, FAN Tian-bo, NAN He, LIU Yun-yi. Preparation of lamellar Mg(OH)<sub>2</sub> with caustic calcined magnesia through apparent hydration of MgO [J]. Industrial & Engineering Chemistry Research, 2013, 52(38): 13661–13668.
- [5] LI Xue, SHI Tong-xin, CHANG Peng, HU Han, XIE Jia-yang, LIU Yun-yi. Preparation of magnesium hydroxide flame retardant from light calcined powder by ammonia circulation method [J]. Powder Technology, 2014, 260: 98-104.
- [6] XIONG Yang, WU Bin, ZHU Jia-wen, FAN Xian-guo, CAI Ping-xiong, WEN Jun, LIU Xiang. Preparation of magnesium hydroxide from leachate of dolomitic phosphate ore with dilute waste acid from titanium dioxide production [J]. Hydrometallurgy, 2014, 142: 137–144.
- [7] SHEN Xiao-yi, WANG Yuan, LIU Yan, DING Ji-wen, ZHAI Yu-chun, WANG Ming-hua. Preparation of spherical flower-like Mg(OH)<sub>2</sub> from waste magnesite and its immobilization performance for Cu<sup>2+</sup>, Zn<sup>2+</sup> and Pb<sup>2+</sup> [J]. Water Science and Technology, 2020, 82(11): 2536–2544.
- [8] SUN Wen-han, DAI Shu-juan, LUO Na, YU Lian-tao. Decalcification leaching test of magnesite based on

- solubleness difference of minerals [J]. The Chinese Journal of Nonferrous Metals, 2019, 29(8): 1733–1739. (in Chinese)
- [9] ZHAO Yu-na, ZHU Guo-cai. A technology of preparing honeycomb-like structure MgO from low grade magnesite [J]. International Journal of Mineral Processing, 2014, 126: 35–40.
- [10] SHEN Xiao-yi, SHAO Hong-mei, LIU Yan, ZHAI Yu-chun. Extraction, phase transformation and kinetics of valuable metals from nickel-chromium mixed metal oxidized ore [J]. Minerals Engineering, 2021, 161: 106737.
- [11] WANG R C, ZHAI Y C, WU X W, NING Z Q, MA P H. Extraction of alumina from fly ash by ammonium hydrogen sulfate roasting technology [J]. Transactions of Nonferrous Metals Society of China, 2014, 24(5): 1596–1603.
- [12] ZHANG Du-chao, REN Guan-xing, LIU Ruo-lin, CHEN Lin, LIU Wei-feng, YANG Tian-zu. Selective separation of zinc and iron from zinc leaching residue by ammonium sulfate roasting [J]. The Chinese Journal of Nonferrous Metals, 2021, 31(7): 1944–1951. (in Chinese)
- [13] BIAN Zhen-zhong, FENG Ya-li, LI Hao-ran. Extraction of valuable metals from Ti-bearing blast furnace slag using ammonium sulfate pressurized pyrolysis-acid leaching processes [J]. Transactions of Nonferrous Metals Society of China, 2020, 30(10): 2836–2847.
- [14] TANG Yi-qi, ZHANG Bei-lei, XIE Hong-wei, QU Xin, XING Peng-fei, YIN Hua-yi. Recovery and regeneration of lithium cobalt oxide from spent lithium-ion batteries through a low-temperature ammonium sulfate roasting approach [J]. Journal of Power Sources, 2020, 474: 228596.
- [15] LI Jin-hui, CHEN Zhi-feng, SHEN Bang-bo, XU Zhi-feng,

- ZHANG Yun-fang. The extraction of valuable metals and phase transformation and formation mechanism in roasting—water leaching process of laterite with ammonium sulfate [J]. Journal of Cleaner Production, 2017, 140: 1148–1155.
- [16] MU Wen-ning, CUI Fu-hui, HUANG Zhi-peng, ZHAI Yu-chun, XU Qian, LUO Shao-hua. Synchronous extraction of nickel and copper from a mixed oxide—sulfide nickel ore in a low-temperature roasting system [J]. Journal of Cleaner Production, 2018, 177: 371–377.
- [17] WANG Wei, GU Hui-min, ZHAI Yu-chun, DAI Yong-nian. New "green" technology of preparing high-purity Mg(OH)<sub>2</sub> from low-grade magnesite [J]. Refractories, 2009, 43: 42–44. (in Chinese)
- [18] LI Yan-chun, LIU Hui, PENG Bing, MIN Xiao-bo, HU Min, PENG Ning, YUANG Ying-zhen, LEI Jie. Study on separating of zinc and iron from zinc leaching residues by roasting with ammonium sulphate [J]. Hydrometallurgy, 2015, 158: 42–48.
- [19] ZHANG Guo-quan, LUO Dong-mei, DENG Chen-hui, LV Li, LIANG Bin, LI Chun. Simultaneous extraction of vanadium and titanium from vanadium slag using ammonium sulfate roasting—leaching process [J]. Journal of Alloys and Compounds, 2018, 742: 504–511.
- [20] YIN S, ALDAHRI T, ROHANI S, LI C, LUO D M, ZHANG G Q, YUE H R, LIANG B, LIU W Z. Insights into the roasting kinetics and mechanism of blast furnace slag with ammonium sulfate for CO<sub>2</sub> mineralization [J]. Industrial & Engineering Chemistry Research, 2019, 58(31): 14026–14036.

# 采用(NH<sub>4</sub>)<sub>2</sub>SO<sub>4</sub> 焙烧-水浸工艺提高菱镁矿的利用效率

申晓毅 1,2, 黄彦翔 1, 邵鸿媚 3, 刘 岩 1, 顾惠敏 1,2, 翟玉春 1

- 1. 东北大学 冶金学院 多金属共生矿生态化冶金教育部重点实验室, 沈阳 110819;
  - 2. 东北大学 辽宁省冶金传感器及技术重点实验室, 沈阳 110819;
    - 3. 沈阳理工大学 环境与化学工程学院, 沈阳 110159

摘 要:研究采用硫酸铵焙烧—水浸工艺提高菱镁矿的利用效率,结合 XRD 和 TG-DTA 分析以及对比硫酸铵焙烧 MgO 的物相变化得到焙烧过程中矿相的转化过程。实验结果表明,在菱镁矿粒度为~74 μm、硫酸铵与菱镁矿物料摩尔比为 1.6:1、焙烧温度为 475 ℃和焙烧时间为 2 h 的条件下,镁的提取率达到 98.7%。反应中物相转化过程可以概括如下: MgCO₃ 先转变为(NH₄)₂Mg₂(SO₄)₃,再分解得到 MgSO₄。反应遵循化学反应和扩散混合控制机理,其表观活化能为 33.02 kJ/mol。

关键词:菱镁矿;硫酸铵焙烧-水浸法;反应过程;物相转化

(Edited by Wei-ping CHEN)